28/04/2024 08:26

(Article begins on next page)

Spin Filtering in Electron Transport Through Chiral Oligopeptides

Spin Filtering in Electron Transport Through Chiral Oligopeptides

M. Kettner[a], B. Göhler, H. Zacharias[*]

Physikalisches Institut, Westfälische Wilhelms-Universität Münster, D-48149 Münster, Germany

D. Mishra[a], V. Kiran, R. Naaman,[*]

Department of Chemical Physics, Weizmann Institute of Science, Rehovot 76100, Israel

Claudio Fontanesi

University of Modena, Department of Chemistry, Via Campi 183,4 1100 Modena , Italy

David H. Waldeck,

Department of Chemistry, University of Pittsburgh, Pittsburgh, PA 15260 USA.

Sławomir Sęk, Jan Pawłowski, Joanna Juhaniewicz

Faculty of Chemistry, Biological and Chemical Research Centre, University of Warsaw, 02-089 Warsaw, Poland

Abstract

We report on the observation of chirality induced spin selectivity for electrons transmitted through monolayers of oligopeptides, both for energies above the vacuum level as well as for bound electrons and for electrons conducted through a single molecule. The dependence of the spin selectivity on the molecular length is measured in an electrochemical cell for bound electrons and in a photoemission spectrometer for photoelectrons. The length dependence and the absolute spin polarization are similar for both energy regimes. Single molecule conductance studies provide an effective charge transport barrier between the two spin channels and it is found to be on the order of 0.5 eV.

a)   Contributed equally

Corresponding author: email: ron.naaman@weizmann.ac.il

Tel:+972-8-9342367

1

1. INTRODUCTION

In recent years it has been shown that electrons transmitted through chiral molecules show a preferred longitudinal spin orientation, an effect referred to as chirality induced spin selectivity (CISS).[1] Detailed experiments which include the analysis of the electron spin orientation and the spin-dependent single-molecule conduction have been carried out so far only for a few cases like double-stranded oligo DNA,[2,3,4] for bacteriorhodopsin,[5] and for photosystem I.[6] A number of theoretical models have been suggested for explaining the high spin polarization observed.[7-17] Despite these efforts, several important questions remain open regarding the origin of the CISS effect. Perhaps the major one is the size of the splitting between the spin states that are related to the electron conduction through the chiral system and the origin for the spin filtering. It is important to appreciate that large spin orbit coupling by itself does not provide spin filtering properties.[17] The vast majority of the models presented rely on a spin-orbit coupling (SOC) value exceeding that of a free carbon atom, ~3.6 meV, and certainly exceeding the spectroscopic values reported for hydrocarbons, which are smaller by one to three orders of magnitude. Another open question is the relation between the molecular structure and its CISS effect.

In this work, we provide additional data on the CISS properties of molecules by extending the observation of the CISS effect to oligopeptides, for both bound electrons and for electrons with energies above the vacuum level. Spin selectivity is observed by three different methods: photoelectron spectroscopy, electrochemistry, and single molecule conduction. The results allow the direct comparison of spin selectivity obtained for bound and unbound electrons and facilitate comparison to previous CISS observations in DNA. The difference in charge transport barrier height for the two spins is directly determined from the conductance measurements. Furthermore, the role of the molecular helical structure in the spin selectivity is assessed by measuring the spin-dependent transmission as a function of helix length and by comparing molecules that retain their α-helix structure to those in a denatured state.

2

1
2
3
4
5
6
7
8
9
10
11
12
13
14
15
16
17
18
19
20
21
22
23
24
25
26
27
28
29
30
31
32
33
34
35
36
37
38
39
40
41
42
43
44
45
46
47
48
49
50
51
52
53
54
55
56
57
58
59
60

2. EXPERIMENTAL METHODS AND MATERIALS

Three different α-helix structured oligopeptides molecules were synthesized by a solid-phase synthesis technique with cysteamine 4-methoxytrityl resin.[18] Their general formula is (Boc)-Cys-(S-Acm)-(Ala-Leu)$_n$-NH-(CH$_2$)$_2$-SH referred to as AL5, AL6, and AL7 for n=5,6,7 respectively. They were used for the preparation of self-assembled monolayers (SAMs) on gold and nickel substrates.

Au and Ni thin films of thickness 150nm were deposited in an e-beam evaporator. The Ni films were reduced electrochemically to remove the oxides before exposing them to the thiolated oligopeptides. The monolayers were characterized as described in the supplementary information and in reference 18 and 19.

2.1 Monolayer adsorption

(Boc)-Cys-(S-Acm)-(Ala-Leu)$_n$-NH-(CH$_2$)$_2$-SH (n = 5−7) molecules of different length were synthesized and their characterization, including helical structure determination, has been reported elsewhere.[18] Prior to the immobilization of a self-assembled monolayer, Au thin films were boiled in acetone and ethanol for 10 minutes each followed by exposing it to the ultraviolet ozone cleaning system for 10 minutes for removing organic contaminants. Then the as-treated Au samples were warmed in ethanol for 20 minutes. The samples were dipped in 0.1 mM solutions of peptides (AL5, AL6 and AL7) in TFE/H$_2$O (6:4 v/v) for 72 and 24 hours for Au and Ni thin films. Ni was reduced electrochemically to facilitate better monolayer formation in a glove box in a high purity nitrogen atmosphere devoid of oxygen content. Prior to the electrochemical reduction of the pristine oxide layer formed on Ni, the Ni substrates were boiled in acetone and ethanol for 20 minutes each. The electrochemical reduction was carried out at -1.0 V versus SCE (Saturated Calomel Electrode, reference electrode) for 20 minutes in 1M HClO$_4$ aqueous solution.[3] After the reduction, the Ni electrode was rinsed immediately in acetone and ethanol to remove the acid and to prevent formation of a new oxide layer. The Ni substrates were never dried or exposed to air prior to the adsorption of the oligopeptide.

2.2 Electrochemistry

Electrochemical measurements were performed by cyclic voltammetry (Biologic) technique. The monolayer coated Ni sample forms the working electrode while Pt acts as

3

counter electrode. A saturated calomel electrode was used as the reference electrode. The redox couple selected for the current study was 3.8mM $K_4[Fe(CN)_6]/K_3[Fe(CN)_6]$ (Fe^{2+}/Fe^{3+}) due to its robust thermodynamic and electrochemical parameters. The Ni thin film was coated with peptide monolayer (AL5, AL6 and AL7) and attached to the bottom of a Teflon cell with an O-ring seal of 0.8 cm inner diameter. The Teflon cell used in the electrochemical experiments was cleaned by carefully washing in "piranha solution." A permanent magnet of field strength H= 0.35T was placed just below the working electrode before the measurements were conducted. The magnetic field strength on the peptide coated Ni surface was measured by a digital Gauss meter. The direction of the magnetic field was changed without disturbing the position of the sample surface of the working electrode exposed to the electrolyte. Details of the electrochemical set up can be found in the ref. 5.

2.3 Single molecule measurements

A schematic of the single molecule measurement is shown in Figure 5 (inset), following previous studies.[3,20,21] Oligopeptides were self-assembled onto a Ni surface as described earlier (section 2). Five nm gold nanoparticles (Sigma Aldrich) were anchored on the outer end of the peptide.[18] The measurements were carried out using a Multimode SPM with Nanoscope controller (Bruker-Nano, Santa Barbara, CA USA). A PtIr-coated Si probe (Bruker, SCM-PIT, spring constant 1-5 N/m) was used. Peak force TUNA (PF-TUNA)[TM] mode was used for acquiring AFM images. In PF-TUNA mode, the tip taps on the surface at a frequency of 1 kHz, controlling the peak contact force (here, held to few nN) at each tap. The tip simultaneously scans the surface at a rate of 1 Hz per scan line. After the adsorption of the oligopeptide on the Ni surface, a topographic scan was performed to establish the density of the gold nanoparticles (GNPs) before performing the I-V measurements. The nanoparticles comprised approximately 60-70% of the image. I-V spectroscopy measurements were recorded by performing voltage ramps with the tip in contact with the surface at an applied force of approximately 10 nN. In this technique, the tip is brought to the surface at a pre-set force. Using the ramping software, the tip was lifted between spectroscopy points at different places on the surface. 10-15% of the spectra exhibited shorting behavior and a similar fraction exhibited insulating behavior. These curves were not used in the analysis. At least 30 I-V curves were averaged for each

4

3. RESULTS AND DISCUSSION

Unbound Electrons: Spin orientation was measured for photoelectrons transmitted through an oligopeptide self-assembled monolayer (SAM) adsorbed on a Au substrate. Three different oligopeptides, with the general formula (Boc)-Cys-(S-Acm)-(Ala-Leu)$_n$-NH-(CH$_2$)$_2$-SH, were studied and are referred to as AL5, AL6, and AL7 for n=5,6,7 respectively (see SI for details on oligopeptide synthesis, film preparation, and characterization). The experimental system for measuring the spin polarization was described previously.[2,5] UV radiation (λ = 213 nm) with photon energy below the ionization potential of the adsorbed oligopeptide molecules, but above the work function of the substrate, was used to excite photoelectrons in the substrate. After these photoelectrons propagated through the layer of the adsorbed molecules, they were analyzed in the vacuum with regard to their spin orientation, using a Mott polarimeter.[22]
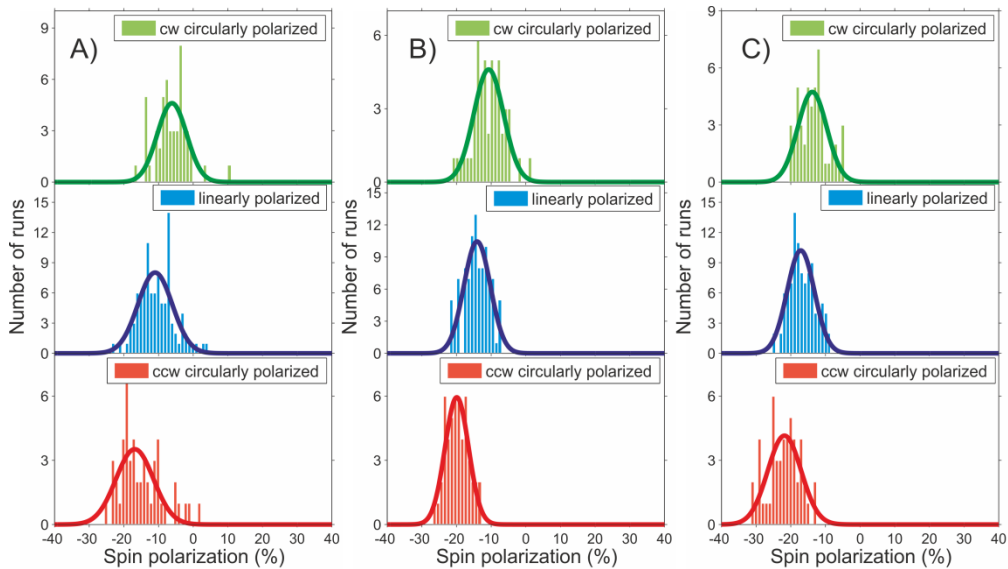

Figure 1: The spin polarization distributions obtained from photoelectron experiments for 2.2 nm (panel A), 2.5 nm (panel B) and 2.8 nm (panel C) long oligopeptides are shown for three different polarizations of the exciting light: clockwise circularly polarized (green), linearly polarized (aqua), and counter-clockwise circularly polarized (red).

5

Figure 1 presents the spin polarization data obtained for photoelectrons transmitted through the AL5, AL6, and AL7 (panels A through C respectively) oligopeptide SAMs on a gold surface. The spin polarization is defined as $P = \frac{I_+ - I_-}{I_+ + I_-}$ where I_+ and I_- are the intensities of electrons with spin orientation parallel or anti-parallel to their velocity, respectively; i.e. in the case of a negative spin polarization (Fig. 1) the majority of detected electrons have a spin oriented antiparallel to their direction of propagation. The quantization axis in this experiment is the electron velocity. The measured spin polarization values range from -11 % (for a 2.2 nm oligopeptide layer) to -17% (for a 2.8 nm oligopeptide layer), when excited with linearly polarized light. If circularly polarized radiation is applied, the electron ensemble, excited in the substrate, is already initially slightly spin polarized (±4% for cw and ccw circular polarized light) before passing through the SAM (see ref.2). Therefore, as the sign of this initial spin polarization depends on the helicity of exciting light (cw or ccw), the measured distributions of spin polarization are shifted accordingly. These variations may indicate that the spin filtering is not ideal, or that some electrons did not pass through the helical molecules.

Bound Electrons: For electron energies below the vacuum level, two independent experimental methods were exploited. Voltammetry was used to measure the magnetic-field dependence of the electron transfer through the oligopeptide SAM in an electrochemical cell. Here, SAMs of the same molecules used in the photoelectron studies were adsorbed on a Ni substrate that served as the working electrode. Pt was used as the counter electrode and a saturated calomel electrode was used as a reference electrode. Cyclic voltammetry measurements were performed as a function of the magnetic field orientation that was applied to the Ni working electrode in order to reveal how the faradaic current through the Ni/SAM interface depends on the magnetization of the supporting Ni.

Figure 2 (A, B, and C) presents the current versus voltage (*I-V*) plots for SAMs of the oligopeptides on Ni. The redox couple was 3.8 mM $K_4[Fe(CN)_6]/K_3[Fe(CN)_6]$ in a 0.4 M KCl aqueous electrolyte, for which the iron changes between the +2 and +3 oxidation states. The value of the peak current decreases with increasing length of the

6

SAM molecules; however the voltammogram appears more 'reversible' for the longer peptide than for the two shorter ones. For AL7 (Fig. 2C), the voltammogram has well-defined cathodic and anodic peaks with a 108 mV separation (a fully reversible couple would be 58 mV), and for the shorter peptides it is 156 mV (AL6) and 151 mV (AL5).[23]
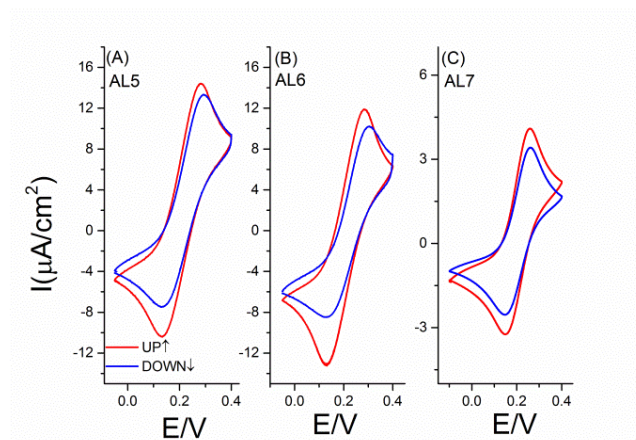

Figure 2: Cyclic voltammograms for the 3.8 mM $K_4[Fe(CN)_6]$/ $K_3[Fe(CN)_6]$ redox couple in a 0.4 M KCl supporting electrolyte, aqueous solution; initial potential = -0.05 V, final potential = +0.4 V, scan rate = 50 mV/s. The working electrode is Ni covered with a self-assembled monolayer of polypeptides (A) AL5, (B) AL6, and (C) AL7. Red and blue curves indicate the two directions (conventionally UP and DOWN, respectively) of the magnetic field (H = 0.35 T), which is normal to the surface of the working electrode.

These variations could reflect differences in the film structure, packing, and other features of the surface which are difficult to control from sample to sample. The quantitative analysis is focused on current variations induced by inverting the magnetic field direction (red and blue curves in Fig 2) for each individual electrode (sample preparation), rather than the absolute magnitude. A magnetic field of 0.35 T was applied parallel (blue curve) and antiparallel (red curve) to the electrode substrate's normal. The data reveal that the current (for both the oxidation and reduction processes) depends on the direction of the applied magnetic field, and this change is robust between the three SAM types and from sample to sample. A similar behavior has also been reported for bacteriorhodopsin coated Ni.[7]

Cyclic voltammograms were measured also for a monolayer of AL6 on a Ni electrode before and after denaturation of the peptide α-helix structure (Figure 3). The

denaturation was caused by heating (adding hot electrolyte solution) and involves the loss of the α-helix structure. The current through the monolayer drops dramatically following the denaturation and spin selectivity is no longer evident. AFM measurements reveal a significant increase in the average thickness of the oligopeptide film upon denaturation. These data indicate that the secondary structure of the polypeptide plays an important role both in its electron transmission properties and in its role as a spin filter.
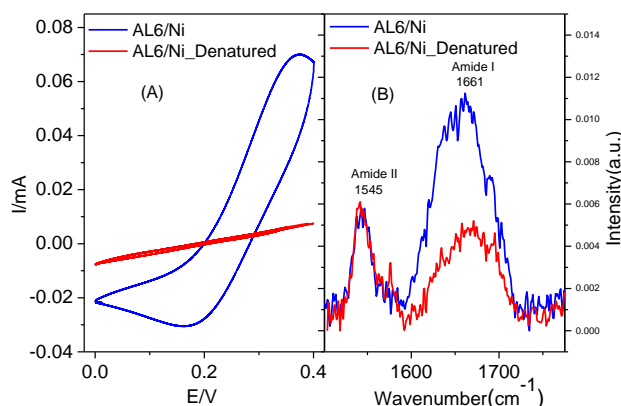

Figure 3: A) Voltammograms are shown for the case of a Ni electrode that is coated with a self-assembled monolayer of oligopeptide AL6 before (blue) and after (red) denaturation. The redox couple is ferricyanide/ferrocyanide; see text. No magnetic field effect was observed for the denaturated oligopeptide. B) The IR spectra are shown for the same monolayer before (blue) and after (red) denaturation. The ratio between the amide I and amide II peaks is reduced dramatically upon denaturation and the amide I peak red shifts upon denaturation, indicating that the molecules are no longer oriented perpendicular to the surface upon denaturation.

Figure 4 shows the dependence of the photoelectron spin polarization on the length of the oligopeptide for the three different incident light polarizations in the photoemission experiment and for the cyclic voltammetry experiment. See Table S1 and Figure S2 for a description of the peptide length determination. Over this short range of distances the polarization increases approximately linearly in magnitude as the length of the oligopeptide increases. Note that the photoelectron's spin polarization is negative and the ccw laser polarization gives the most negative spin polarization for a given oligopeptide length. The data reveal a weak dependence of the photoelectron spin polarization on the initial polarization of the laser pulse. This result is consistent with earlier data on

8

monolayers of double stranded DNA.[2] For the cyclic voltammetry data, the polarization is defined as the magnitude of the current with magnetic field pointing parallel (UP) to the electrode's surface normal minus the magnitude of the current measured with the magnetic field pointing anti-parallel to the electrode's surface normal (DOWN) divided by their sum.
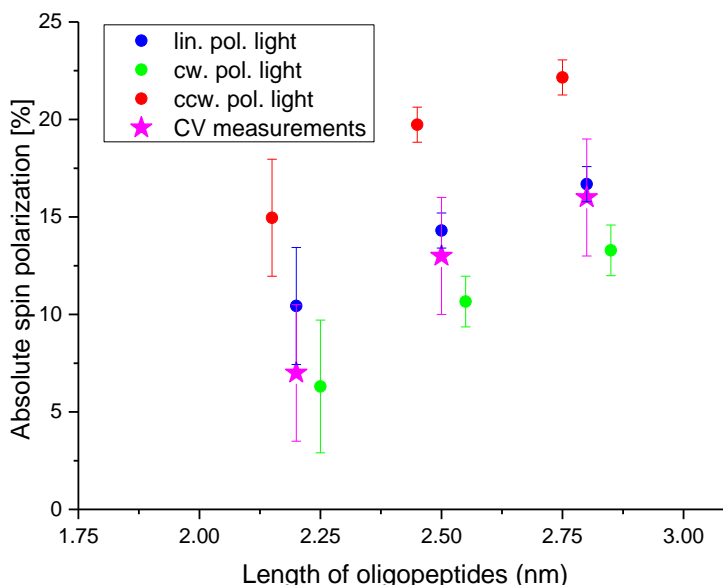

Figure 4: The length dependence of the absolute value of the longitudinal spin polarization. The results for the photoelectrons are shown for clockwise and counter clockwise circular polarized (green and red respectively) and for linear polarized light (blue). The spin polarization, in the electrochemical study, of the faradaic current at 0.13 V and 0.28 V is shown as pink stars. The sign of the polarization in the photoelectron signal was negative, while in the case of the electrochemical studies it was not determined.

The current used for these comparisons is that recorded at 0.13 V and 0.28V on the cathodic and anodic scan respectively. Unlike the photoemission studies, information on the actual spin orientation in the lab frame, hence the sign of the polarization, is not available; however, the data show that the magnitude of the polarization increases with the oligopeptide length, from 8% for AL5 (2.2 nm) to 17% for AL7 (2.8nm). The lengths given here correspond to the end-to-end distance of the oligopeptide molecules. It is worth noting that these oligopeptides are more efficient spin filters than DNA on a per unit length basis. While a spin polarization of 9% has been reported for an 8.8 nm long (26 base pairs) ds DNA; the oligopeptides studied here are only 2.2 nm in length and have a spin polarization of 8%.

Measurements of spin dependent conduction through single molecules was performed in a setup similar to that described in references 3 and 20. A monolayer of the oligopeptide was formed on a Ni substrate, gold nanoparticles were adsorbed on top of the oligopeptide, and conductive AFM was used to measure the current (I) versus voltage (V) curves as a function of the magnetization direction of the Ni substrate.

Figure 5 shows current vs voltage curves for AL7, and the dI/dV plot which indicates the density of states. The ratio in current between the two spins, when measured at 0.7 V, is about one order of magnitude, indicating highly efficient spin filtering. The difference in the energy between the two spin states is given by the differences in the band gaps of the spin density of states, as shown in the insert of Fig. 4, which amounts to 0.5±0.1 eV.

The high selectivity measured here as compared to that found in the photoemission and electrochemical analysis may indicate that in the other methods, electrons emitted from uncovered areas of the surface reduce the overall spin polarization measured. In the single molecule study, no such background electrons exist and hence the "true" spin selectivity of the molecule is measured.
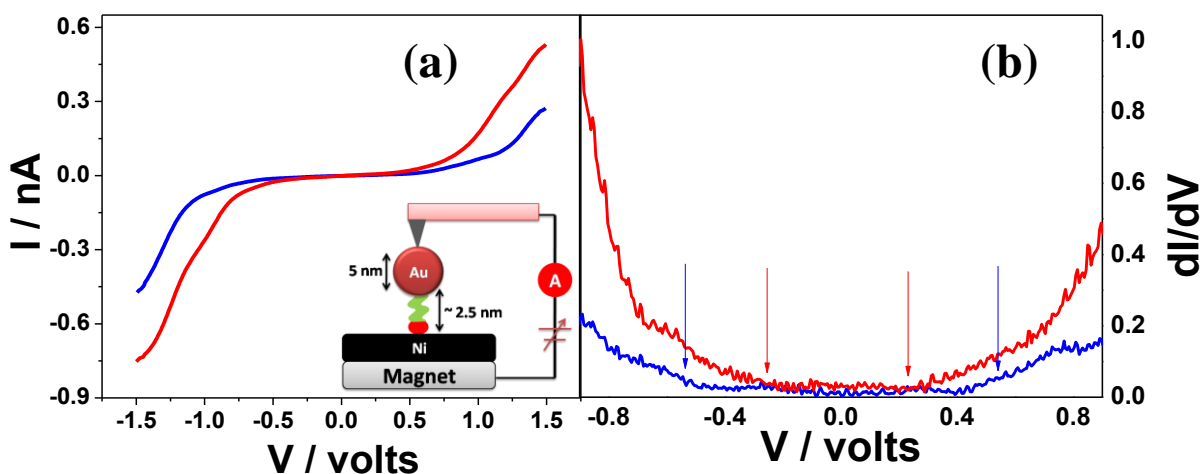

Figure 5: (a) Current (I) versus voltage (V) measured by conductive AFM through an AL7 molecule adsorbed on Ni substrate. The measurements were conducted with the magnetic moment of the Ni substrate pointing up (blue) or down (red). Inset shows schematic illustration of the device structure. (b) The plot of dI/dV, providing the density of states. The energy gaps are noted by blue and red arrows for spin up and down respectively.

In conclusion, we presented new measurements on electron transfer and efficient spin filtering (the CISS effect) by monolayers and single molecule of oligopeptides at

room temperature. The data establish the dependence of the efficient electron transfer through the oligopeptides and of the efficient spin filtering on the oligopeptides secondary (α-helix) structure. The results clearly indicate that the CISS effect is robust and is not very sensitive to the environment in which the chiral molecule is imbedded. The results are similar for "dry" (in vacuum or in ambient) and "wet" monolayers (in electrochemical cell). The spin filtering efficiency per unit length exceeds that of DNA reported before, by more than a factor of two. As with earlier studies, the CISS effect requires an unusually large splitting of the spin states for electrons propagating through a helical potential. The accumulated experimental results indicate that for electrons moving through a chiral potential, the system has unusual "spintronic" properties.

Supporting Information

The supporting information includes details on the material used, on the adsorption of the molecules and on the characterization of the self-assembled monolayers formed.

Acknowledgements

References:

[1] Naaman, R.; Waldeck, D.H. Chiral-induced Spin Selectivity Effect. *J. Phys Chem. Lett*. **2012,** *3*, 2178-2187.

[2] Göhler, B.; Hamelbeck, V.; Markus, T.Z.; Kettner, M.; Hanne, G.F. ; Vager, Z.; Naaman, R.; Zacharias, H. Spin Selectivity in Electron Transmission Through Self-Assembled Monolayers of Double-Stranded DNA. *Science* **2011,** *331*, 894-897.

[3] Xie, Z.; Markus, T. Z. ; Cohen, S. R.; Vager, Z.; Gutierrez, R.; Naaman, R. Spin Specific Electron Conduction Through DNA Oligomers. *Nano Lett*. **2011,** 11, 4652-4655.

[4] Ravi S.; Sowmiya P.; Karthikeyan, A. Magnetoresistance And Spin-Filtering Efficiency of DNA-Sandwiched Ferromagnetic Nanostructures. *Spin* **2013**, *3*, 13500031-1350034.

[5] Mishra, D.; Markus, T.Z.; Naaman, R.; Kettner, M.; Göhler, B.; Zacharias, H.; Friedman N.; Sheves, M.; Fontanesi, C. Spin-Dependent Electron Transmission Through Bacteriorhodopsin Embedded in Purple Membrane. *Proc. Natl. Acad. Sci. USA,* **2013,** *110*, 14872-14876.

[6] Carmeli, I.; Kumar, K. S.; Hieflero, O.; Carmeli, C.; Naaman, R. Spin Selectivity in Electron Transfer in Photosystem I. *Angew. Chem. Int. Ed.* **2014**, *126*, 9099-9104.

[7] Yeganeh, S.; Ratner, M. A.; Medina, E.; Mujica, V. Chiral Electron Transport: Scattering Through Helical Potentials *J. Chem. Phys*. **2009,** 131, 014707.

[8] Medina E.; Lopez, F.; Ratner, M. A.; Mujica, V. Chiral Molecular Films as Electron Polarizers and Polarization Modulators. *EPL* **2012,** *99*, 17006.

12

[9] Gutierrez, R.; Díaz, E.; Naaman, R.; Cuniberti, G. Spin-Selective Transport Through Helical Molecular Systems. *Phys. Rev. B* **2012,** *85*, 081404.

[10] Gutierrez, R.; Díaz, E.; Gaul, C.; Brumme, T.; Domínguez-Adame, F. ; Cuniberti, G. Modeling Spin Transport in Helical Fields: Derivation of an Effective Low-Dimensional Hamiltonian. *J. Phys. Chem. C* **2013,** *117*, 22276-22284.

[11] Guo, A.-M.; Sun, Q.-F. Spin-Selective Transport of Electrons in DNA Double Helix. *Phys. Rev. Lett.* **2012,** 108, 218102.

[12] Guo, A. M.; Sun, Q. F. Sequence-Dependent Spin-Selective Tunneling Along Double-Stranded DNA. *Phys. Rev. B* **2012,** *86,* 115441.

[13] Rai, D.; Galperin, M. Electrically Driven Spin Currents in DNA. *J. Phys. Chem. C* **2013,** *117,* 13730-13737.

[14] Gersten, J.; Kaasbjerg, K.; Nitzan, A. Induced Spin Filtering In Electron Transmission Through Chiral Molecular Layers Adsorbed on Metals With Strong Spin-Orbit Coupling. *J. Chem. Phys.* **2013,** *139*, 114111.

[15] Vager, D.; Vager, Z. Spin Order Without Magnetism – A New Phase Of Spontaneously Broken Symmetry in Condensed Matter. *Phys. Lett. A* **2012,** *376***,** 1895-1897.

[16] Kuzmin S.L.; Duley, W.W. Properties of Specific Electron Helical States Leads to Spin Filtering Effect in dsDNA Molecules. *Phys. Lett. A* **2010,** *378*,1647-1650.

[17] Guo, A.-M.; Sun, Q.-F. Spin-Dependent Electron Transport in Protein-Like Single-Helical Molecules *Proc. Natl. Acad. Sci.* **2014,** *111*,11658-11662.

[18] Pawlowski, J.; Juhaniewicz, J.; Tymecka, D.; Sek, S. Electron Transfer Across α-Helical Peptide Monolayers: Importance of Interchain Coupling. *Langmuir* **2012,** 28, 17287-17294.

[19] Carmeli, I.; Skakalova, V.; Naaman R.; Vager Z. Magnetization of Chiral Monolayers of Polypeptide-A Possible Source of Magnetism in Some Biological Membranes, *Angew. Chem. Int. Ed.* **2002,** 41, 761-764.

[20] Nogues, C.; Cohen, S. R.; Daube, S. S; Naaman R. Electrical Properties of Short DNA Oligomers Characterized by Conducting Atomic Force Microscopy. *Phys. Chem. Chem. Phys*. **2004,** *6*, 4459-4466.

13

[21] Nogues, C.; Cohen, S.R.; Daube, S. S.; Apter, N.; Naaman R. Sequence Dependence of Charge Transport Properties of DNA. *J. Phys. Chem. B* **2006,** *110***,** 8910-8913.

[22] Mott, N. F. Scattering of Fast Electrons by Atomic Nuclei. *Proc. R. Soc. A* **1929,** *124,* 425-442; ibid **1932,** *135,* 429.

[23] Note that the positive 0.4 V value, in the CV curves, is a limit due to the start of the Ni electrochemical oxidation active at more positive potentials, as it was determined in screening experiments.

TOC: